ICP-1128
SEPTEMBER 1977

PHYSICAL PROPERTIES AND HEAT TRANSFER CHARACTERISTICS OF MATERIALS FOR KRYPTON-85 STORAGE

Allied Chemical
IDAHO CHEMICAL PROGRAMS

IDAHO NATIONAL ENGINEERING LABORATORY

ENERGY RESEARCH AND DEVELOPMENT ADMINISTRATION

IDAHO OPERATIONS OFFICE UNDER CONTRACT EY-76-C-07-1540

Printed in the United States of America
Available from
National Technical Information Service
U.S. Department of Commerce
5285 Port Royal Road
Springfield, Virginia 22161
Price: Printed Copy $5.25; Microfiche $3.00

ICP-1128

ICP-1128
Distributed Under Category:
UC-70
Nuclear Waste Management
TID-4500, R65

PHYSICAL PROPERTIES AND HEAT TRANSFER CHARACTERISTICS OF MATERIALS FOR KRYPTON-85 STORAGE

by

A. B. Christensen

Date Published - September 1977

ALLIED CHEMICAL CORPORATION
IDAHO CHEMICAL PROGRAMS - OPERATIONS OFFICE

Prepared for
ENERGY RESEARCH AND DEVELOPMENT ADMINISTRATION
IDAHO OPERATIONS OFFICE
UNDER CONTRACT EY-76-C-07-1540

ABSTRACT

Krypton-85 decay results in heat generation, and the subsequent temperature increase in the krypton-85 storage media must be evaluated. This report compiles the physical properties of krypton and of potential krypton-85 storage materials which are required to calculate the maximum temperature developed during storage. Temperature calculations were made for krypton-85 stored as a gas or immobilized solid in steel storage cylinders. The effects of krypton-85 loading, cylinder radius, storage media properties, and exterior cooling on storage temperature were shown.

SUMMARY

Collection and storage of ∿85% of the krypton-85 produced by nuclear fuel reprocessing is required by Federal regulations for fuel irradiated after 1982. Krypton can be stored as a gas in pressurized cylinders or immobilized either in granular materials, such as zeolites, or in monolithic amorphous or crystalline metals prior to storage. The safety of the storage system depends on the temperatures resulting from the radioactive decay heat generation. For example, a temperature increase in a ^{85}Kr-pressurized cylinder not only increases the gas pressure, but may reduce the wall strength, resulting in possible cylinder failure and release of radioactive krypton. This report compiles the necessary physical properties of krypton and of potential krypton-85 storage materials which are required to evaluate the maximum temperatures developed during storage.

Krypton volumetric data in the pressure and temperature ranges of 0-200 MPa and 273-423 K, respectively, were fitted to the Redlich-Kwong (R-K) equation of state. Krypton thermal conductivity data were correlated in the 0.1-95 MPa and 273-608 K ranges. Heat generation and decay rates were given as a function of time.

Granular thermal conductivities depend on the thermal conductivities of the solid and of its surrounding gas, and on the void fraction. Granular thermal conductivities increase with temperature and pressure, but decrease with void fraction; a correlation fitted 76% of the data with an error of ± 30%. Thermal conductivity, density, void fraction, mean particle diameter, and sorbed-water concentration at room temperature and pressure are tabulated for zeolites; thermal conductivities of silicate, borosilicate and borate glasses, and of aluminum, nickel, copper, and iron are given. Since no thermal conductivity data exist for amorphous metals, values intermediate to glass and metal were assumed.

Maximum temperatures were calculated (assuming natural convection cooling in air) for a single horizontal cylinder containing krypton-85 fixed in solids or as a gas, and for storage cells containing 104 cylinders. Cylinders containing krypton-85 as a pressurized gas or in crystalline metals yielded the lowest maximum storage temperatures for a given radius and loading. Void fraction changes in granular materials loaded with krypton-85 weakly influenced the maximum temperature. The effects of natural convection cooling of a cylinder in air and water were compared.

Further calculations should be made for different storage configurations such as annular cylinders or cylinders with cooling fines. Maximum temperatures in underground storage media should be estimated. Experiments should be performed to verify the calculations.

CONTENTS

APPENDICES

TABLES

FIGURES

1.0 INTRODUCTION

Several isotopes of krypton and xenon are produced in a nuclear reactor. Essentially all of these gaseous isotopes remain trapped in the fuel rods and are freed only with the dissolution of the rods.[1] A lag time of 160 days between reactor shutdown and fuel rod reprocessing allows all of these isotopes to decay to stable states except for krypton-85. Krypton-85 has a half-life of 10.7 years, a power output per unit mass of 0.574 W/g and is chemically stable. Krypton-85 decays through a beta emission to the stable rubidium-85 isotope.

Fuel reprocessing plants could become the dominant source of krypton-85 in the atmosphere.[1] Due to its chemical stability, krypton-85 leaves the atmosphere only through radioactive decay. Since krypton-85 is biologically inert, the critical dosage to a human is to the skin. Release of krypton-85 from reprocessing plants could cause a hundred-fold increase in present atmospheric krypton-85 dose levels.[1]

Krypton-85 is currently being released at reprocessing plants. An available collection method is cryogenic distillation. This process has been operated intermittently at the Idaho Chemical Processing Plant (ICPP) since 1958 for research and industrial applications. An alternative is fluorocarbon absorption, which has been in pilot plant operation since 1975. Federal regulations require krypton-85 collection and storage of at least 86% of the krypton-85 produced by commercial nuclear reactors after 1982.[2] At present, the only storage method available is the containment of krypton-85 in high-pressure cylinders.[3] Other methods being developed include high pressure and temperature encapsulation in zeolites or glasses and ion implantation/sputtering in crystalline or amorphous solids.[3,4] The storage reliability of gas cylinders depends on the wall temperature and gas pressure. The diffusion of krypton-85 out of zeolites, glasses, or metals depends directly on the temperature. The transfer rate of the krypton-85 decay heat and resulting temperature profiles in these storage forms must be known for evaluating long-term storage effectiveness.

This report describes those physical properties of krypton, krypton-85, and of the solid materials which are important in calculating the storage temperature. Heat transfer calculations are made for krypton-85 storage in gaseous and solid forms in isolated cylinders, and for groups of cylinders in storage cells.

2.0 PHYSICAL PROPERTIES OF KRYPTON AND KRYPTON-85

The decay rate and the heat generation of krypton-85 are required for the temperature distribution calculations of krypton-85 storage systems. Pressure-volume-temperature (P-V-T) and thermal conductivity data are also required for these calculations. These data were taken from the literature and fitted to tested analytical correlations for interpolation and extrapolation of the data.

2.1 Heat Generation by Krypton-85 Decay

Krypton-85 has a half-life of 10.73 years. The equation for its decay is:

$$N = 0.06 \cdot N_0 \cdot \exp(-0.0646 \cdot t) \quad (1)$$

where N is the number of moles of krypton-85 remaining after t years and N_0 is the initial number of moles of krypton containing 6 vol% krypton-85. The decay scheme for krypton-85 follows two paths: 99.57% of all disintegrations give beta and the rest give gamma radiation. The maximum and average decay energies are 0.687 and 0.24[6] Mev per disintegration, respectively. The rate equation of the decay energy release, E, for 6 vol% krypton-85 in krypton is:

$$E = 2.9 \cdot N_0 \cdot \exp(-0.0646 \cdot t) \quad (2)$$

where E is in watts. The decay rate of krypton-85 as a function of time is:

$$\frac{dN}{dt} = 74 \cdot N_0 \cdot \exp(-0.0646 \cdot t) \quad (3)$$

where $\frac{dN}{dt}$ is in terabecquerels (TBq). Figure 1 shows the decrease in heat generation rates with time.

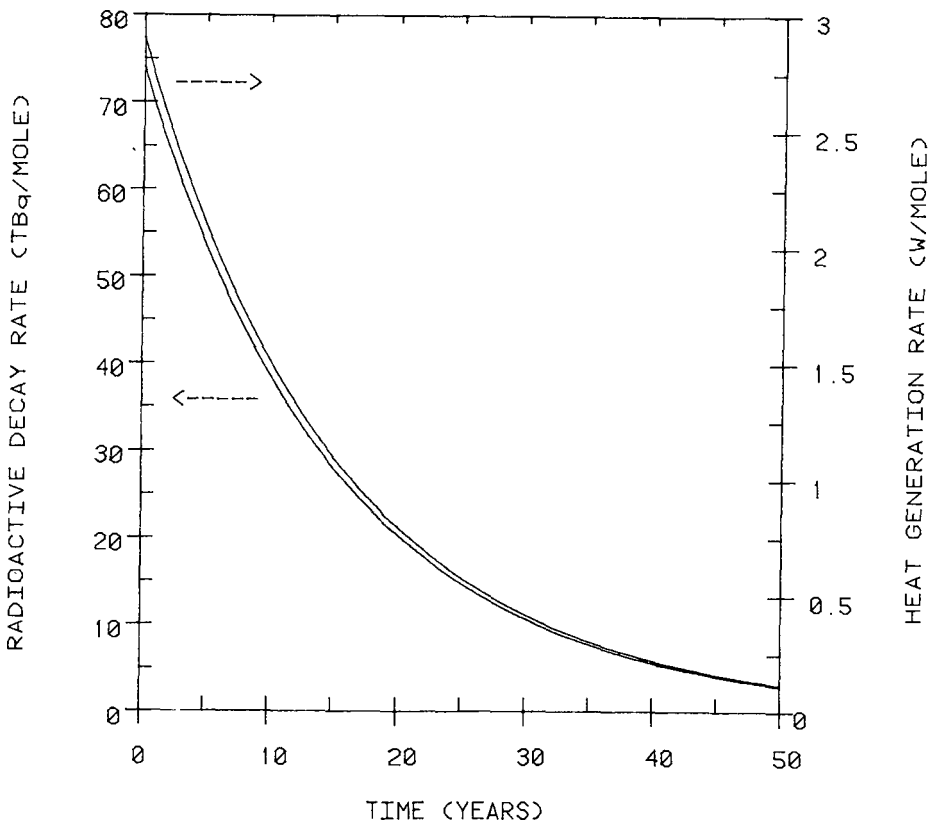

Figure 1. Krypton-85 heat generation and decay rates as a function of time.

2.2 Pressure-Volume-Temperature Properties of Krypton

The pressure-volume-temperature data for krypton must be described in terms of an equation of state for interpolation and extrapolation of the data. The two-parameter Redlich-Kwong (R-K) equation (Equation 4) is superior to several multiparameter equations.[5]

$$P = \frac{RT}{v-b} - \frac{a}{v(v+b)} \qquad (4)$$

where P is the pressure, T is the temperature, v is the specific volume, R is the universal gas constant, and a and b are constants. For better accuracy, a and b are regarded as temperature dependent. The parameters, a and b, were correlated from the available data[6,7,8,9] for P in MPa,

T in Kelvin, v and b in $cm^3 \cdot mol^{-1}$, and a in $MPa \cdot cm^6 \cdot mol^{-2}$ using Equations (5) and (6):

$$b = 28.2074 - 1.0485 \times 10^{-4}T \quad (5)$$

$$a = RT(-28.1525 + 6487.6089/T + 5452723.596/T^2 + b) \quad (6)$$

These parameters produce average and maximum percent errors in the data of 1.6 and 5.4%, respectively.

If the specific volume (v) is to be calculated (given P and T), then the cubic polynomial shown below must be solved.

$$v^3 - \frac{RT}{P} v^2 + (\frac{a}{P} - b^2 - \frac{RTb}{P})v - \frac{ab}{P} = 0 \quad (7)$$

The compressibility is equal to Pv/RT and measures the deviation of a gas from its ideal state. Figure 2 shows compressibility isotherms of krypton, calculated using Equations (5) and (6), as a function of pressure.

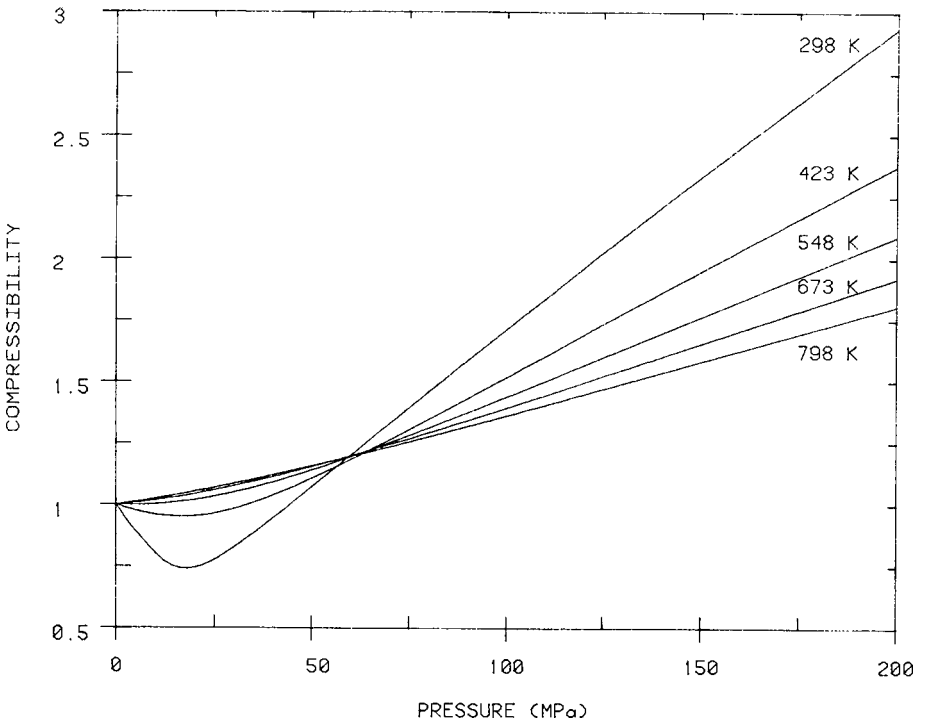

Figure 2. Compressibility isotherms of krypton as a function of pressure.

2.3 Thermal Conductivity of Krypton

The thermal conductivity (k_g) of krypton is a function of temperature and pressure. At low pressure ($\sim$1 MPa), k_g is only a function of temperature and equals k_{go}. Equation (8) gives the thermal conductivity.[10]

$$k_g - k_{go} = cv^d \tag{8}$$

where k_g and k_{go} are units of watts$\cdot$cm$^{-1}\cdot$K^{-1} and v in cm$^3\cdot$mol^{-1}, and k_{go} is a function of temperature only.

Measured values of k_{go} between 350 and 1500 K fit the parabolic equation:

$$k_{go} = 1.993 \times 10^{-5} + 2.65 \times 10^{-7}\cdot T - 3.72 \times 10^{-11}\cdot T^2 \tag{9}$$

with an absolute deviation of $\pm$ 0.2% from the data.[11] Using measured[12] data for k_g in the ranges 294 - 608 K and 0.1 - 95 MPa and Equation (9), the fitted constants for Equation (8) were found to be:

$$c = 3.4717 \times 10^{-2}$$

$$d = -1.2121$$

Figure 3 shows krypton thermal conductivity isotherms calculated from Equation (8) as a function of pressure.

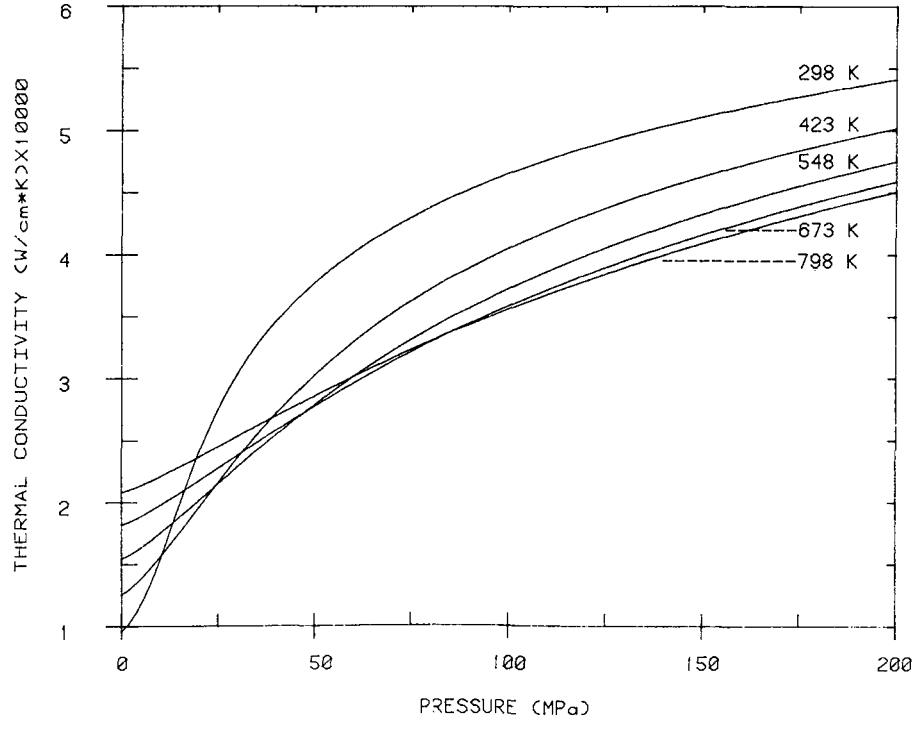

Figure 3. Thermal conductivity isotherms of krypton as a function of pressure.

3.0 EFFECTIVE THERMAL CONDUCTIVITY OF GRANULAR MEDIA

Since there is no good correlation for estimating solid thermal conductivities, it must be found experimentally. The effective thermal conductivity (k_e) for granular materials is a function of the solid conductivity (k_s), the conductivity of the fluid surrounding the solids (k_g), and the void fraction (ε) of the solids. The effects of these variables on the effective material conductivity (k_e) have been measured.[13,14,15,16] Above 800 K, heat transfer due to radiation becomes significant and the effective conductivity must be corrected for conductivity due to radiation (k_r).[15] The effects of fluid medium, temperature, pressure, void fraction, convection currents, and radiation on k_e are discussed in the following section.

3.1 Effect of Fluid Medium Surrounding Granular Material

The effective conductivity of stainless steel powder with three different gases is shown in Figure 4.[14] The ratio of k_g of helium to argon at 370 K is 8.08; the ratio of k_e at the same temperature for these gases is 3.65.

Because of the low thermal conductivity of the gas phase most of the heat transfer will occur near the contact points of the granules.

3.2 Effect of Temperature

The functional relationship of temperature on effective conductivity (Figure 4) is linear over the temperature range. As the gas becomes heavier, the functional dependence on temperature weakens.

3.3 Effect of Pressure

Figure 5 shows the effect of pressure on k_e for magnesium oxide powder[14] At low pressures, this effect is strongest. Pressure changes of the surrounding gas medium will not affect k_e above a certain "breakaway pressure." According to kinetic theory, the mean free path of a gas molecule at the breakaway pressure becomes small compared to the intergranular distances and increases in the thermal conductivity with pressure are negligible.

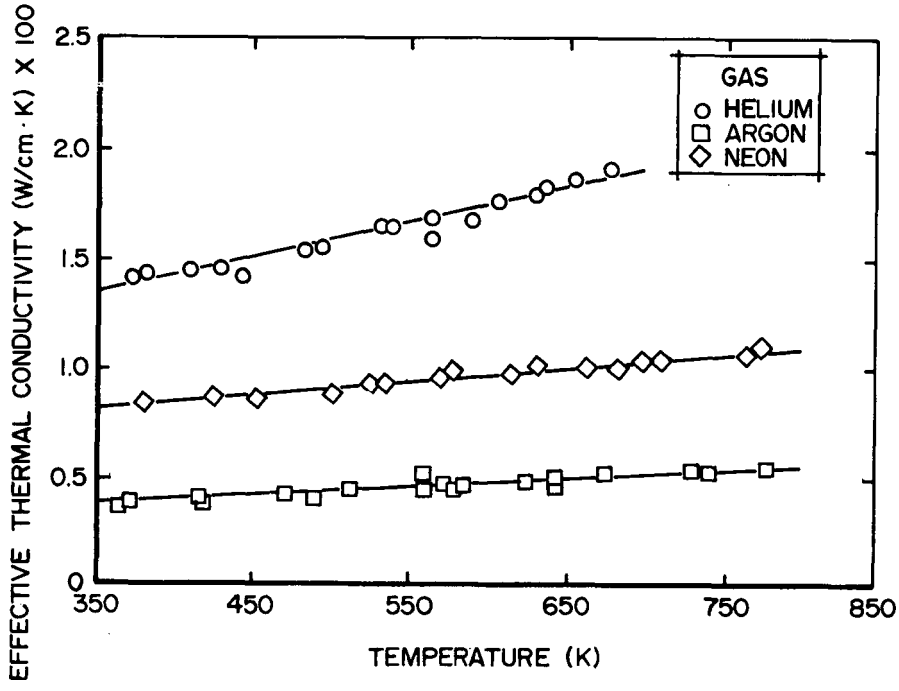

Figure 4. Effect of temperature and gas type on effective thermal conductivity for stainless steel powder[14]

3.4 Effect of Void Fraction

Figure 6 shows the void fraction effects on effective conductivity.[14] Thermal conductivities are measured for blocks of solid aluminum oxide with regular arrays of holes, and k_e decreases linearly with increasing void fraction.[16]

3.5 Effect of Convection Currents

Heat transfer by induced convection currents is small if the granules are less than one centimetre in diameter.[15]

3.6 Effect of Radiation

Above 800 K, the radiation conductivity, k_r, is given by

$$k_r = 1.3956 \times 10^{-7} d_w C \left(\frac{T}{100}\right)^3 \qquad (10)$$

where d_w is the average grain diameter in millimetres and C is the material emissivity factor (dimensionless).

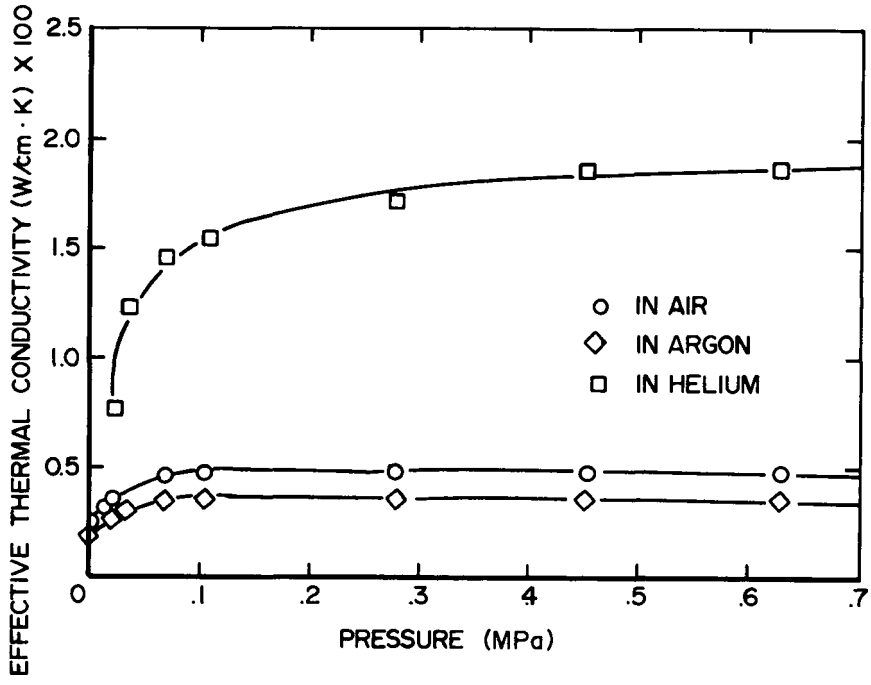

Figure 5. Effect of gas pressure on effective thermal conductivity of magnesium oxide powder.[14]

3.7 Correlation of Effective Thermal Conductivity for Granular Materials

The best available correlation[15] is of the form:

$$\frac{k_e}{k_g} = \left(\frac{k_s}{k_g}\right)\left[A + B \log \left(\frac{k_s}{k_g}\right)\right] \qquad (11)$$

where A is a function of void fraction, the correlated values A and B are:

$$A = 0.28 - 0.757 \log (\varepsilon) \qquad (12)$$

$$B = -0.057 \qquad (13)$$

Since the gas occupying the granular void space acts as an insulator, most of the heat transfer occurs near points of contact between the

particles of solid in the granular mixture. As the gas thermal conductivity decreases, the area at these contact points, and the contact point geometry becomes important in calculating the granular thermal conductivity. Equation (11) fails for low values of Kg such that $K_S/K_g \geq 500$.

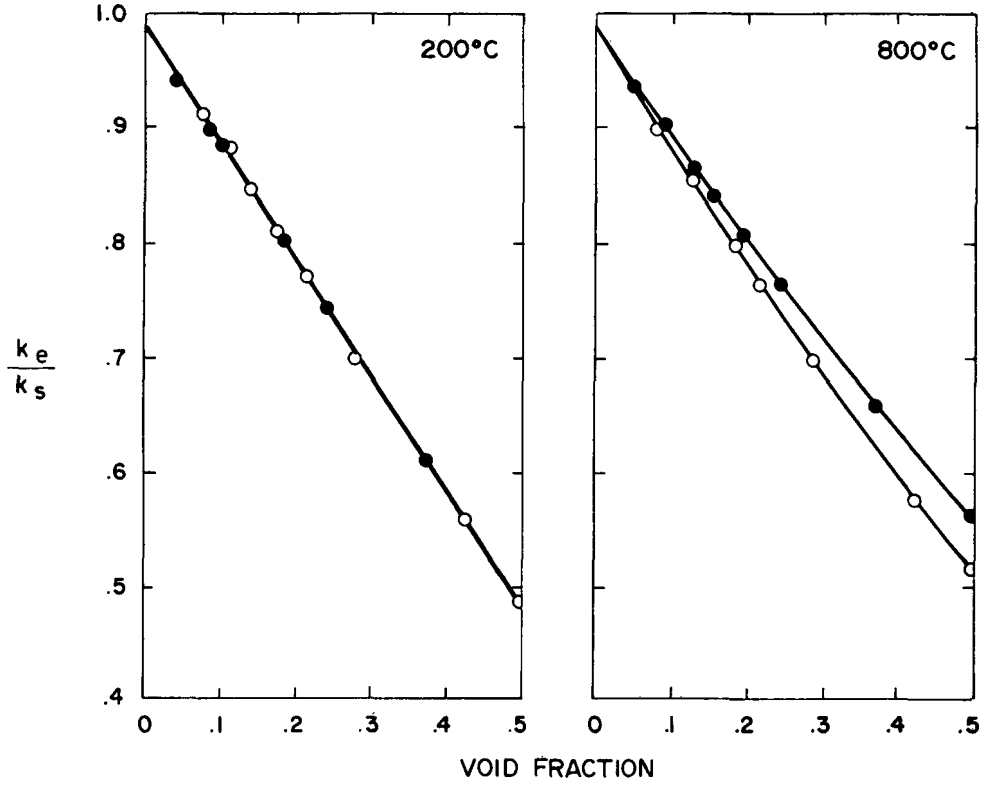

Figure 6. Effect of void fraction on effective thermal conductivity of aluminum oxide.[16] Solid and open circles represent pore diameters of 0.146 and 0.082 cm, respectively.

Figure 7 compares the available data using Equation (11).[15] The fitted parameters A and B fall in the void fraction range $0.21 \leq \varepsilon \leq 0.48$, although small extrapolations may be made.

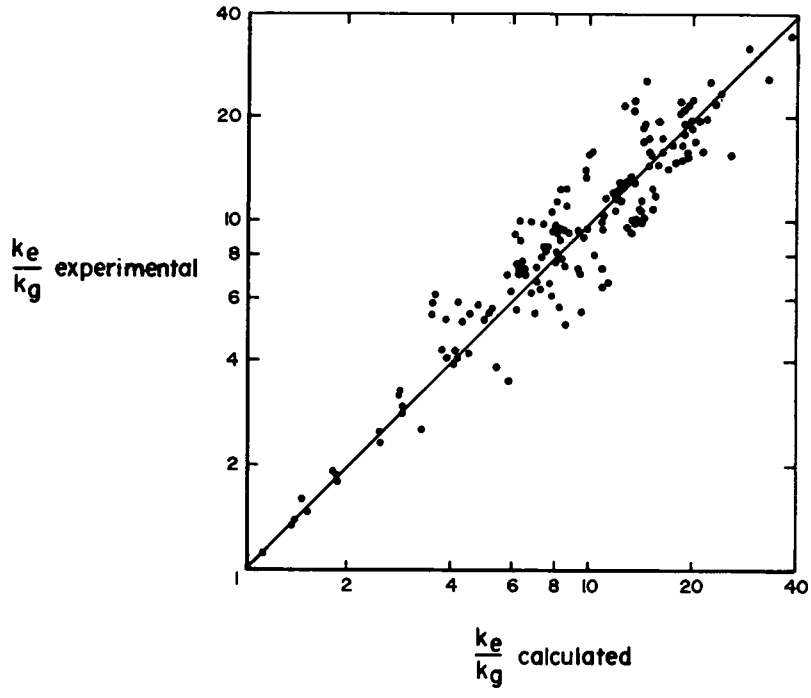

Figure 7. Comparison of experimental with calculated effective thermal conductivities of granular materials[15]

4.0 EFFECTIVE THERMAL CONDUCTIVITY OF ZEOLITES

Zeolite effective thermal conductivities were measured as a function of temperature, and k_e values were converted to k_s values using Equation (11). The resulting k_s values were fitted to a straightline function in temperature, because of its suitability to low-conducting solids.[13,14] An extrapolation beyond the temperature range of the thermal conductivity data was necessary for some of the temperature calculations.

A Dynatech C-Matic was used to measure thermal conductivities. The thermal conductivities were taken using ambient air (at 0.1 mPa) filling the void space.

4.1 Effect of Sorbed Water

Zeolite thermal conductivity increases with water sorption. Figure 8 shows thermal conductivity data for activated (baked under vacuum at 673 K to drive out the water) and unactivated 3A zeolites at different temperatures.

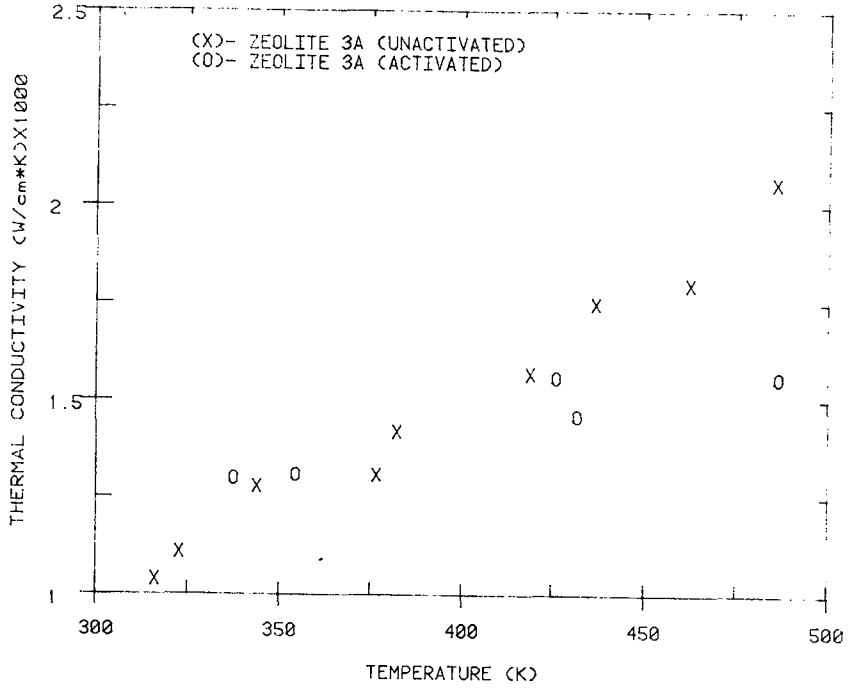

Figure 8. Effect of water sorption on effective thermal conductivity of zeolite 3A.

Zeolite-3A with sorbed water has higher thermal conductivities than zeolite without water. Since sorbed water amount decreases with increasing temperature, zeolite thermal conductivity may decrease above 500 K.

4.2 Effect of Pill Binder

Leached sodalite was pilled using two kinds of binder: a 2% graphite and a 2% graphite-10% alumina mixture. Both were found to have thermal conductivities that increased at the same rate with temperature. Sodalite-alumina pills show higher thermal conductivities than sodalite pills. Data for sodalite-alumina and sodalite pills may be used to show that the thermal conductivity of a solid mixture may be estimated using Equation (14), which is based on a mass fraction average of the component thermal conductivities:

$$k_{mix} = \sum_{i=1}^{N} k_i X_i \qquad (14)$$

where k_i is the component thermal conductivity and x_i its mass fraction in the solid, k_{mix} is the mixture thermal conductivity, and N is the number of components in the mixture. The solid thermal conductivities for sodalite with 2% graphite and for alumina are 5×10^{-3} and $1.3 \times 10^{-2} W \cdot cm^{-1} \cdot K^{-1}$, respectively, using Equation (14).

$$(0.9)(5 \times 10^{-3}) + (0.1)(1.3 \times 10^{-2}) = 5.8 \times 10^{-3}$$

Thermal conductivity value for a solid mixture with 10% alumina and 90% sodalite is $6 \times 10^{-3} W \cdot cm^{-1} \cdot K^{-1}$.

4.3 Effect of Void Fraction

Figure 9 shows the porosity effect on thermal conductivity. Pilled zeolites are shown to have higher conductivities than powdered zeolites. Pilled and powdered zeolites normally have a void fraction of $\sim$0.4 and $\sim$0.6, respectively. Since pill breakage causes a reduction in the void fraction of a bed, an increase in thermal conductivity is expected for zeolite beds with large amounts of pill breakage.

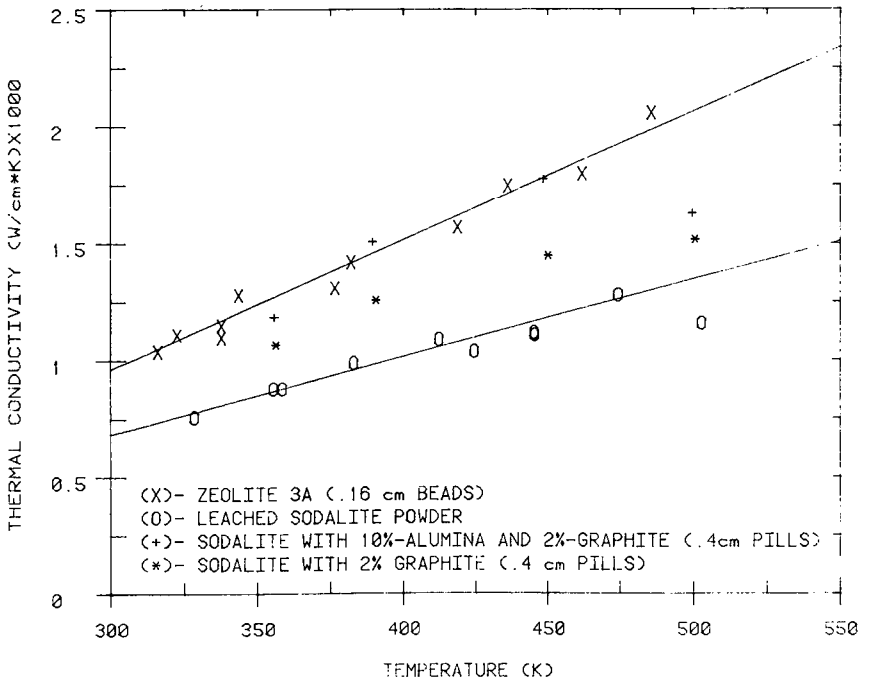

Figure 9. Effect of void fraction on effective thermal conductivity of zeolites

4.4 Physical Properties of Zeolites

Characteristics which are important for heat transfer include water loading, average particle dimension, and bulk, particle, and absolute density. Pilled zeolite needs two void fractions (ε) to describe the total voidage. ε_1 is the void fraction around the pills, and ε_2 describes that fraction inside the pill. ε_1 and ε_2 may be calculated using Equations (15) and (16).

$$\varepsilon_1 = 1.0 - \frac{\text{Bulk Density}}{\text{Particle Density}} \tag{15}$$

$$\varepsilon_1 = 1.0 - \frac{\text{Particle Density}}{\text{Absolute Density}} \tag{16}$$

where bulk density is the density of a settled bed of pilled zeolite, particle density is the density of one pill, and absolute density is the density of crystalline zeolite. Table 1 shows the different densities,

average particle size, and water sorption at room temperature for some zeolites. The densities and particle diameters were obtained at the Idaho National Engineering Laboratory (INEL). Typical water sorptions were found in Breck,[17] and the void fractions were found using Equations (15) and (16).

TABLE 1

PHYSICAL PROPERTIES OF ZEOLITES USED TO ENCAPSULATE KRYPTON

Zeolite	Density, g/cm^3			Void Fraction, %		Avg Particle Diam, mm	Water Loading, g H_2O/g dry solid
	Bulk	Particle	Absolute	Intra-Pellet	Extra-Pellet		
Leached sodalite, pilled with 2% graphite and 10% alumina	0.67	1.143	2.30	50.3	41.38	3.97	0.20
Leached sodalite, pilled with 2% graphite	0.59	1.031	2.25	54.18	42.77	3.97	0.20
Leached sodalite, powdered	0.60	1.72	2.24	78.57	63.95	0.002	0.20
Rubidium-exchanged zeolite A, binderless spheres	0.89	1.55	2.26	31.42	42.58	1.812	0.27
Cesium-exchanged zeolite A, binderless spheres	0.90	1.552	2.33	33.39	42.01	1.756	0.27
Potassium-exchanged erionite, granular	0.69	1.67	2.25	58.68	58.68	1.117	0.22
Potassium-exchanged erionite, powdered	0.65	1.67	2.21	70.59	61.08	0.081	0.22
Potassium-exchanged chabazite, granular	0.57	1.229	2.15	53.62	53.62	1.024	0.27

5.0 PHYSICAL PROPERTIES OF CRYSTALLINE AND AMORPHOUS SOLIDS

5.1 Glass

Encapsulation of krypton is assumed to occur in spherical beads of silicate (100% SiO_2), borosilicate crown (71% SiO_2, 15% B_2O_3), and light borate crown (70% B_2O_3, 18% Al_2O_3) glass. The beads are assumed to be 1.57 mm diameter with a void fraction of 0.476. The densities for the solid and the bulk pellets are given in Table 2.[18]

TABLE 2

BULK AND SOLID DENSITIES FOR SOME GLASSES[18]

Glass Type	Solid Density	Bulk Density for 1.57 mm Spheres
Silica glass	2.20	1.15
Borosilicate	2.37	1.24
Borate crown	2.24	1.17

The thermal conductivity of solid glass increases linearly with temperature over a large temperature range. Extrapolation is valid, because the temperature dependence of k_s is weak. Table 3 gives the values calculated from the data[19] using the equation $k_s = A + B \cdot T$.

TABLE 3

THERMAL CONDUCTIVITY PARAMETERS OF SOME GLASSES*

Glass	A	B	Temp Range, K
Silica	0.01	1.36×10^{-5}	323-773
Borosilicate	5.0×10^{-4}	4.2×10^{-5}	273-409
Borate crown	4.9×10^{-3}	3.11×10^{-5}	273-373

*Calculated from k_s data in Ref. 19, using the equation, $k_s = A + B \cdot T$.

5.2 Crystalline and Amorphous Metals

Krypton-85 can be encapsulated in crystalline and amorphous metals by ion implantation/sputtering techniques. Crystalline nickel, iron, and amorphous gadolinium-cobalt-molybdenum alloys have been used. Thermal conductivity and density values of some crystalline metals are given in Table 4.[20]

TABLE 4

PHYSICAL PROPERTIES OF SOME CRYSTALLINE METALS

Metal	$k(W \cdot cm^{-1} \cdot K^{-1})$	Solid Density $(g \cdot cm^{-3})$
Aluminum	2.05	2.70
Nickel	0.79	8.91
Copper	3.76	8.91
Iron	0.71	7.86

Thermal conductivities of amorphous metals are not known; values in the range 0.01 - 0.1 $W \cdot cm^{-1} \cdot K^{-1}$ have been chosen for calculations (thermal conductivity of glass is 0.01 $W \cdot cm^{-1} \cdot K^{-1}$).

6.0 STORAGE OF KRYPTON-85-LOADED SOLIDS

Once krypton-85 is loaded into zeolite, glass, or metal, it must be contained and stored. Krypton-85 must be stored until at least 99% of it has decayed to a stable state; krypton-85 decay generates heat, resulting in a temperature increase. Since the krypton-85 diffusion rate out of a solid increases with temperature, the storage medium's ability to retain the krypton-85 decreases with increasing temperature.[3] The temperature is dependent on four factors: the volume of krypton stored per volume of solid, the rate of heat conduction through the solid, the heat transfer rate from the vessel to the surroundings.

The maximum temperature inside a cylinder is found using Equation (17):

$$AT_0 + \frac{B}{2}T_0^2 = AT_1 + \frac{B}{2}T_1^2 + \frac{SR_1^2}{4} \qquad (17)$$

where T_0 and T_1 are the centerline and wall temperatures, respectively, S is the volumetric heat generation rate of krypton-85 in $W \cdot cm^{-3}$, R_1 is the inside cylinder wall radius in cm, and A and B are coefficients for calculating effective thermal conductivity. The heat convection from the cylinder wall is assumed to obey Newton's cooling law:

$$Q = hA(T_2 - T_a) \qquad (18)$$

where Q is the heat loss in watts, A is the area of the convecting surface in square centimetres, T_2 and T_a are the outside cylinder wall and bulk fluid temperatures, respectively, and h is the heat transfer coefficient in $W \cdot cm^{-2} \cdot K^{-1}$ with h depending on $(T_2 - T_a)$, the bulk fluid properties and the cylinder diameter. For granular solids, the void fraction is assumed to be filled with air at 0.1 MPa.

This section shows how the above parameters influence T_0 for one cylinder. Maximum temperatures are then calculated for a group of cylinders stored in a storage cell.

6.1 Maximum Storage Temperature Calculations

6.1.1 Effect of Radius and Krypton-85 Loading. The interaction of radius, krypton-85 loading, and centerline temperature is shown in Figure 10 using isotherms and in Figure 11 using lines of constant radius for sodalite pellets with graphite-alumina binding. The void fraction was taken as 0.41, and the bulk density as 0.67 $g \cdot cm^{-3}$ Cylinders are placed horizontally in air at 0.1 MPa and 300 K. From Figure 11, it can be seen that the centerline temperature does not increase linearly with loading, but falls off at increased loadings.

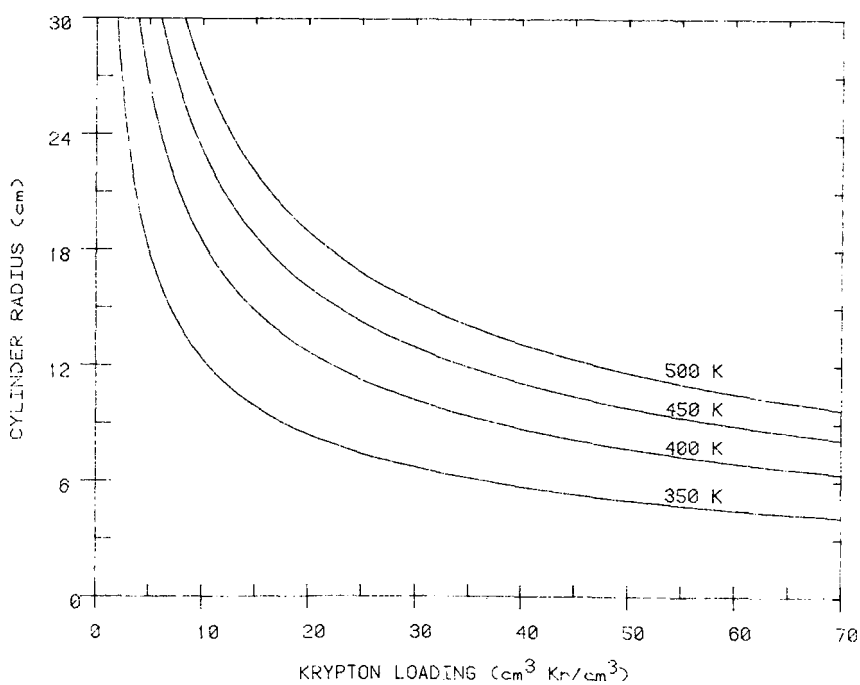

Figure 10. Cylinder radius corresponding to maximum temperatures of 350, 400, 450, and 500 K as a function of krypton loading on pilled zeolite with a void fraction of 0.41; cylinder placed horizontally in air at 300 K

For horizontal cylinders in ambient air at 300 K and with a radius of 11.5 cm, the effect of loading on maximum temperature is shown

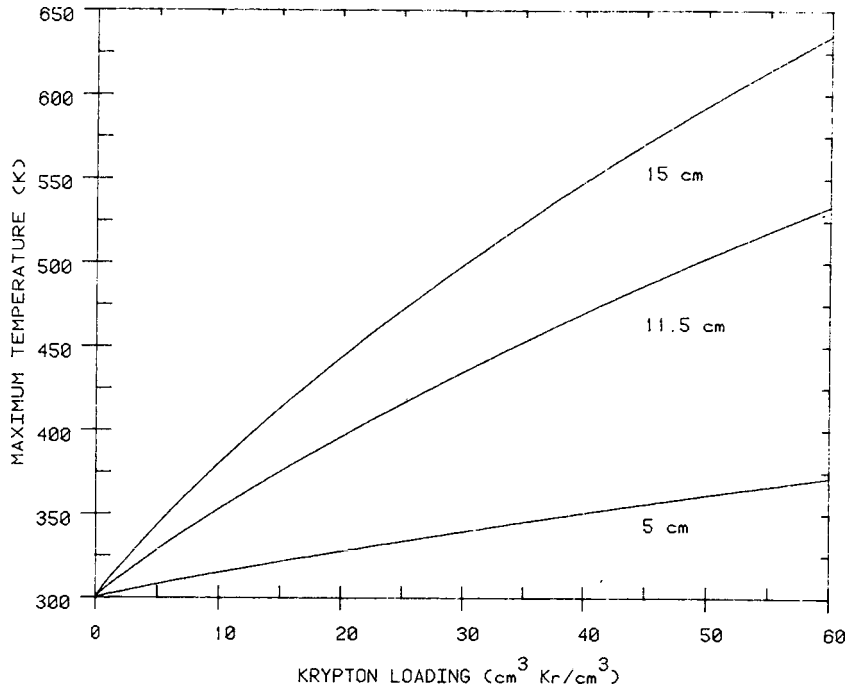

Figure 11. Maximum temperature produced in 10-, 23-, and 30-cm-diam horizontal cylinder in air at 300 K as a function of krypton loading on zeolite pills with a void fraction of 0.41.

in Figures 12 (low loading) and 13 (high loading) for solids capable of loading krypton-85.[4] Krypton-85 stored as a pressurized gas (6% ^{85}Kr in krypton) is included in Figure 12 as a comparison (with loading expressed in STP cm^3Kr/cm^3 container). Since data for physical properties of solids containing encapsulated krypton are not available, the properties of solids containing encapsulated krypton are not available, the properties of the host solid are used; in amorphous metals, the density was assumed to be 7 $g \cdot cm^{-3}$ and the thermal conductivity (k) was assumed to be 0.01 $W \cdot cm^{-1} \cdot K^{-1}$ for Figure 12 and 0.01, 0.05, or 0.1 $W \cdot cm^{-1} \cdot K^{-1}$ for Figure 13. Zeolites, glass, and some metals have not been loaded beyond 100 cm^3 krypton per cm^3 solid; crystalline and amorphous metals have been loaded up to $\sim$140 and $\sim$890 cm^3 krypton cm^3 solid, respectively.[4] For crystalline

metals and the pressurized gas, centerline and wall temperatures were about the same. Granular materials such as zeolite or sintered glass had the highest maximum temperature for a given loading.

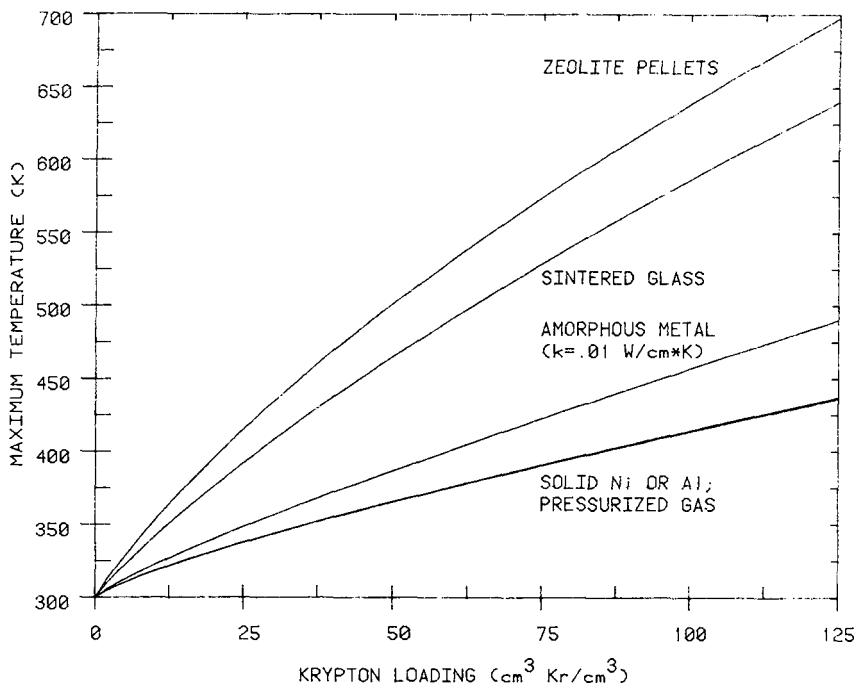

Figure 12. Maximum temperature produced in a horizontal 23-cm-diam cylinder in air at 300 K as a function of krypton loading, 0 - 125 cm^3 Kr/cm^3 solid.

6.1.2 Effect of Void Fraction. The void fraction (ε) indirectly influences the centerline temperature by affecting the thermal conductivity. The void fraction may vary in the range 0.3 - 0.6. The void fraction of a pilled material depends on the pill shape and strength. Figure 14 was calculated using a zeolite pellet with a density of 1.14 $g \cdot cm^{-3}$, a cylinder radius of 15 cm, and a krypton-85 loading of 30 $cm^3 \cdot g^{-1}$. The bulk density was calculated as void fraction varied using Equation (15). The temperature goes through a maximum as ε increases, because of two opposing effects: as ε increases, the solid thermal conductivity increases, but the volumetric heat generation rate (in $W \cdot cm^{-3}$) decreases.

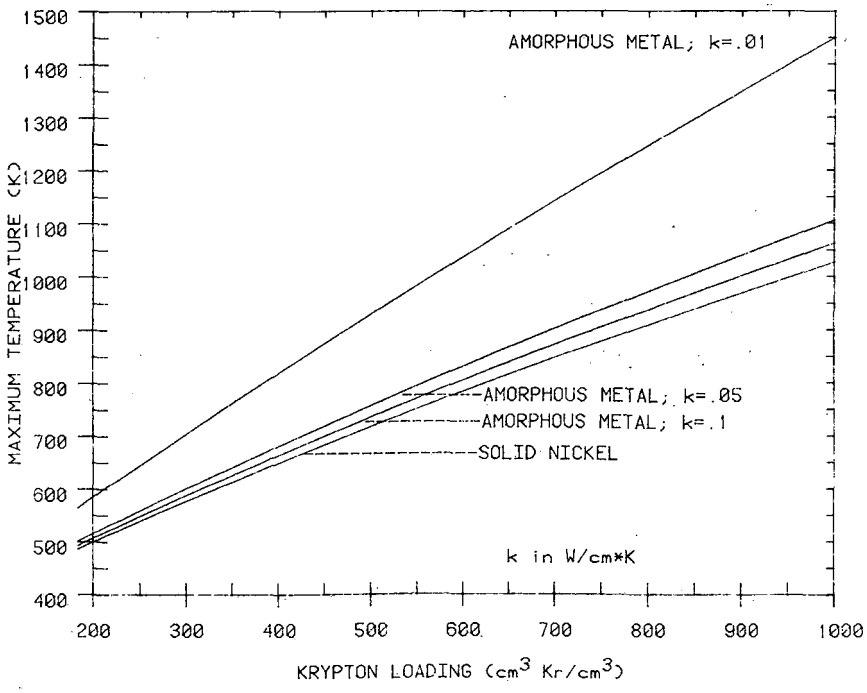

Figure 13. Maximum temperature produced in a horizontal 23-cm-diam cylinder in air at 300 K as a function of krypton loading, 100 to 1000 cm^3 Kr/cm^3 solid.

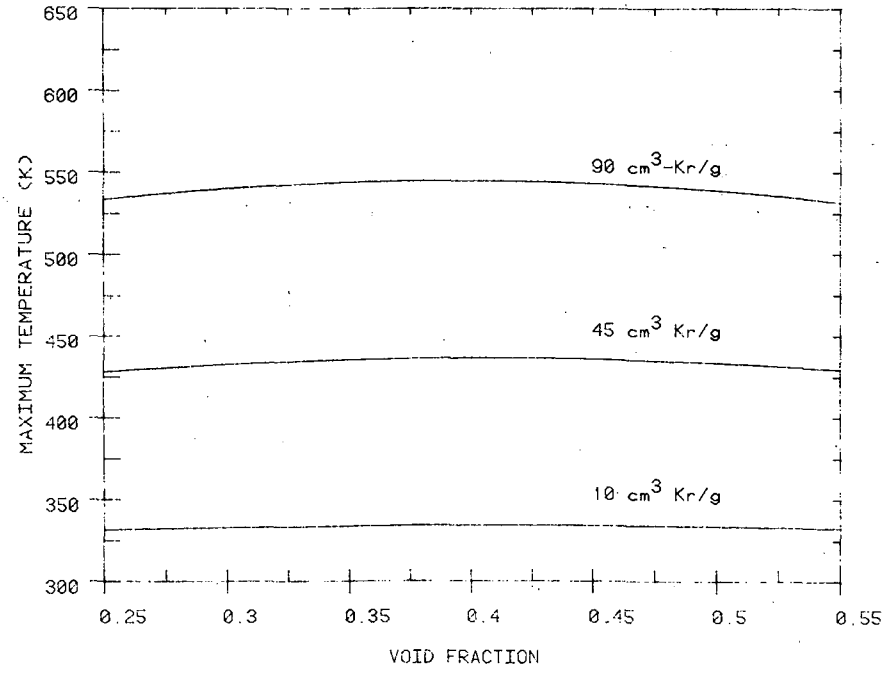

Figure 14. Maximum temperature produced in a horizontal 23-cm-diam cylinder in air at 300 K as a function of void fraction of the pilled zeolite for constant krypton loading.

6.1.3 Effect of Cooling Fluid. Cylinders may be stored in different types of cooling fluids. In this report, only cooling by natural convection is considered, since forced cooling may prove unreliable for long storage times. The cylinders may be stored in water pools or in dry air storage cells.

The storage reliability in water is compared with that in air using cylinders containing pilled zeolite and cooled either in a large pool of water at 300 K or in dry air at 0.1 MPa and 300 K. Assuming the same concentration of krypton-85, the radius of the water-cooled cylinder is 1.11 times that for the air-cooled cylinder, and the storage volume in a cylinder in water is 1.23 times that in air.

The centerline temperature was calculated as a function of cooling medium temperature for air and water. The maximum temperature increases linearly with increasing temperature; however, the maximum temperature of a cylinder cooled in water is 30 K cooler than a cylinder cooled in air at the same temperature as water. Temperatures for cylinders stored in other media can be estimated using the data in this section, since the temperature gradient inside the cylinder is independent of the medium in which the cylinder is stored.

6.2 Cylinder Storage in Cells

A conceptual design for a storage facility provides for horizontal storage of cylinders in externally cooled cells.[21] Calculations were made for natural heat convection from the cell walls to the facility air as the only cooling mechanism. Cell air was considered to be isothermal; facility air was assumed to have a bulk temperature of 318 K. The airtight cell is 19 metres long by 2.4 metres wide by 5.2 metres high; 104 cylinders are stored at equal intervals throughout the cell, approximately one cylinder (49.6 L, 11.5 cm radius) stored per vertical square metre. Table 5 shows cylinder and cell temperatures for zeolite, metal, and glass storage.

TABLE 5

CYLINDER AND CELL TEMPERATURES FOR KRYPTON-85
IMMOBILIZED IN
ZEOLITE, GLASS, AND CRYSTALLINE AND AMORPHOUS METALS,
AND STORED IN HORIZONTAL 23-CM-DIAM CYLINDERS

Kr* Loading	Cell Conditions**		Centerline Temperature for Different Solids, K			
	Temperature, K	Pressure, MPa	Zeolite Pellets	Sintered Glass	Crystalline Metal	Amorphous Metal
15	342	.114	388	387	366	373
25	352	.118	419	417	389	400
40	367	.122	453	452	420	437
50	376	.125	471	470	439	460
100	414	.138	-	-	522	564
500	636	.212	-	-	986	1199

*cm^3 of krypton at STP per cm^3 solid.

**Facility air assumed at 45^oC.

7.0 STORAGE OF KRYPTON-85 IN PRESSURIZED CYLINDERS

Storage of krypton-85 in high-pressure gas cylinders is an available technology. Increased cylinder temperature due to the krypton-85 heat generation may affect storage capacity. For example, carbon steels used in cylinder manufacture exhibit strain aging between 423 and 640 K, with a net increase in tensile strength.[22] Above 640 K, tensile strength decreases with increasing temperature.[22] Furthermore, at constant density, gas pressure increases linearly with temperature; therefore, higher cylinder temperatures result in higher gas pressures. Commercial high-pressure gas cylinders are built according to Department of Transportation (DOT) specifications to withstand 2.5 to 3 times their rated pressure before bursting.[23] Therefore, a cylinder whose DOT specification is 3AA-2400, is 139 cm in length, 22.8 cm in diameter, 49.55 L in volume, and has a rated pressure of 16.3 MPa, will have a possible minimum burst pressure of 40.8 MPa. Cylinder temperature and pressure must be determined from its krypton-85 loading and storage configuration.

7.1 Storage Wall Temperature Calculations

Wall temperatures of cylinders containing gaseous krypton-85 depend on the heat transfer rate from wall to air, and from its storage location to ambient conditions. Pressurized gas is assumed to be the same temperature as the cylinder wall. Calculations were made for a single horizontal cylinder and for a group of cylinders. Cylinder diameter and the cooling air temperature are parameters which influence heat transfer by natural convection. Previous heat transfer calculations, shown in Table 6, assumed radial heat transport and a gas temperature equal to the wall temperature.

For a long vertical cylinder, a temperature gradient exists in the gas.[24] A convection cell is produced, with fluid rising at the center, and falling at the wall. Using a correlation for estimating an effective heat transfer coefficient between gas and wall, an effective gas temperature which is higher than that of the wall is calculated. For horizontal cylinders, such convection cells may exist, but no attempt was made to model them. The following calculations assume horizontal cylinder storage and gas temperature equal to the wall temperature.

TABLE 6

PROPERTIES OF CYLINDERS CONTAINING KRYPTON-85*

Pressure, MPa	^{85}Kr Content, PBq	Heat Generation, W	Wall T,** K
3.4	4.74	187	337
8.6	11.0	434	371
13.8	16.4	647	398

* Assuming DOT-specification 3AA-2400 cylinders (22.8-cm-diam, 49.55 L) containing 6% krypton-85 in krypton.
** Assuming natural convection cooling of horizontal cylinders in air at 300 K.

7.1.1 Effect of Radius. Figure 16 shows the effect of radius on wall temperature for different isobars. For a radius of 15 cm, doubling a 3.4 MPa gas pressure increases the temperature by 42 K. Increasing the pressure by another 3.4 MPa results in a 32 K increase. The radius effect on temperature decreases with increasing radius.

7.1.2 Effect of Cooling Fluid. The results are shown in Section 6.1.3 and also apply to pressurized cylinders.

7.2 Cylinder Storage in Cells

A conceptual design for a cell storing high-pressure cylinders assumed forced cooling.[21] Wall temperatures and pressures were estimated assuming the cell's cooling capacities were lost and cooling occurred through the walls only.[25] Table 7 shows cell and cylinder temperatures and pressures for cylinders containing different amounts of krypton-85.

TABLE 7

CYLINDER AND CELL TEMPERATURES FOR KRYPTON-85
STORED IN HORIZONTAL 23-CM-DIAM STEEL CYLINDERS*

^{85}Kr Content, TBq	Cell		Cylinder	
	Temperature, K	Pressure, MPa	Temperature, K	Pressure, MPa
4 736	357	1.31	398	4.7
9 028	380	1.39	448	13.4
11 026	390	1.43	469	20.1
12 913	399	1.46	488	28.7
16 428	415	1.52	521	52.0

* 104 50-litre cylinders containing 6% krypton-85 in krypton; outside cell temperature at 318 K.

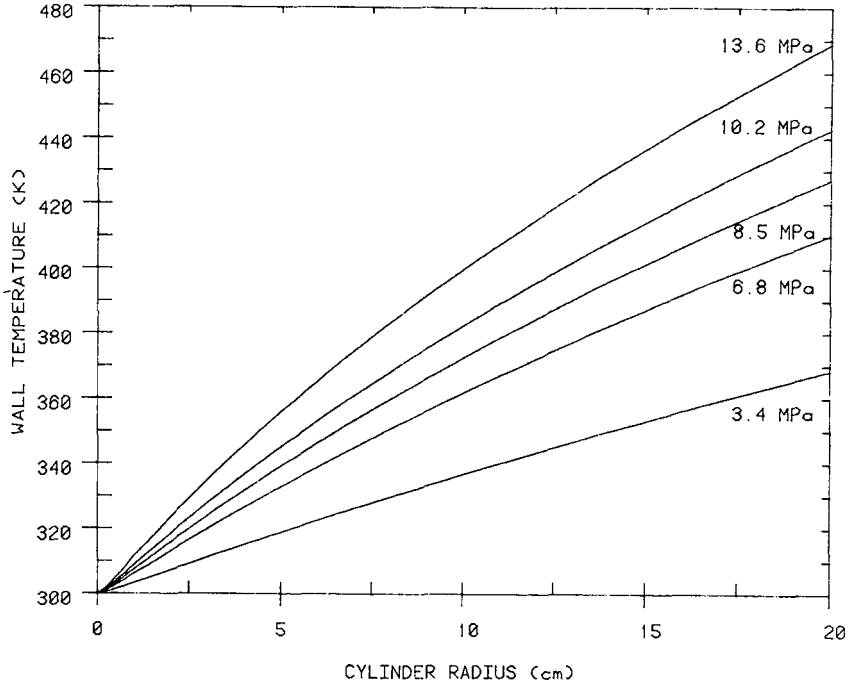

Figure 15. Maximum temperature produced for different isobars of 6% krypton-85 in krypton as a function of radius for a horizontal cylinder in air at 300 K

8.0 CONCLUSIONS AND RECOMMENDATIONS

Maximum temperature calculations should be made for any krypton-85 storage system to determine safety and storage reliability. Although most of the calculations represent a cylinder containing krypton-85 cooled by natural convection to air, results given may be used to calculate the maximum temperature in a cylinder stored in other media. For example, the temperature drop through a cylinder in air is calculated for a given cylinder size and krypton-85 loading. Then, the temperature of the medium is calculated up to the wall for the same heat generation rate. The maximum temperature is the cylinder temperature drop added to the temperature at the wall.

Since little krypton-85 leaks from sodalite at 423 K,[4] loadings up to 30 STP cm^3 Kr/cm^3 solid are allowed for a horizontal 11.5-cm-radius cylinder in air at 300 K (see Figure 12). Observed loadings are 25 cm^3 Kr·cm^{-3} solid.[4] Assuming a maximum temperature of 423 K allows loadings of ∿110 and ∿75 cm^3 Kr·cm^{-3} solid in nickel and amorphous metal (for k = 0.01 W·cm^{-1}·K^{-1}), respectively. The amorphous metal ($Gd_{0.11}$ $Co_{0.73}$ $Mo_{0.16}$) crystallizes and releases Kr at 1073 K.[26] Assuming a thermal conductivity of 0.01 W·cm^{-1}·K^{-1} and storage temperature of 423 K, maximum loading is 650 cm^3 Kr·cm^{-3} solid.

Temperature gradients across solids with thermal conductivities above 0.1 W·cm^{-1}·K^{-1} are not significant. For granular materials, maximum temperatures are not affected by changes in their void fraction (Figure 14). Equation (11) shows that granular thermal conductivities may be increased by surrounding the solid with a high thermal conductivity gas.

Although the Redlich-Kwong parameters (Equation 5 and 6) were found for krypton volumetric data in the temperature range 273 - 423 K, the R-K equation may be used to calculate volumetric data at temperatures up to 900 K.

Gaps exist in the physical data required for storage temperature calculations. Volumetric data for krypton should be measured in the ranges 10 - 200 MPa and 450 - 900 K. Krypton thermal conductivities are required above 100 MPa and 610 K. Thermal conductivities of solids loaded with krypton and of amorphous metals need to be measured.

Other storage modes should be considered. Storage in finned or annular cylinders are two possibilities. For forced cooling of cylinders, steady-state and transient (i.e., post-loss of cooling) maximum temperatures must be calculated.

9.0 REFERENCES

1. National Council on Radiation Protection and Measurements, Krypton-85 in the Atmosphere-Accumulation, Biological Significance, and Control Technology, NRCP Report No. 44, Washington, D.C., July 1, 1975.

2. "Environmental Radiation Protection Standards for Nuclear Power Operations", Federal Register, vol. 42, No. 9, Title 40, Part 190, January 13, 1977.

3. Alternatives for Managing Wastes from Reactors and Post-Fission Operations in the LWR Fuel Cycle, ERDA-76-43, NTIS, Springfield, Va., Ch. 14.1, vol. 2, pp.147-14.7, April 1976.

4. D. A. Knecht, An Evaluation of Methods for Immobilizing Krypton-85, ICP-1125, Idaho National Engineering Laboratory, Idaho Falls, ID, July 1977.

5. K. K. Shaw and G. Thodos, "A Comparison of Equations of State", Ind. Eng. Chem., Vol 57, No. 3, pp 30-37 (March 1965)

6. R. Simonet and E. Behar, "A Modified Redlich-Kwong Equation of State for Accurately Representing Pure Components Data", Chemical Engineering Science, vol. 31, No. 1, pp.37-43 (1976).

7. N. J. Trappeniers, T. Wassenaar, and G. J. Walders, "Isotherms and Thermodynamic Properties of Krypton between 0^{o} and 150^{o} and at Densities up to 620 Amagats", Physica, vol. 32, No. 9, pp.1503-20, 1966.

8. J. A. Beattie, J. S. Brierley, and R. J. Barriault, "The Compressibility of Gaseous Krypton II. The Virial Coefficients and Potential Parameters of Krypton", J. Chem. Phys., vol. 20, No. 10, pp.1615-18, October 1952.

9. E. Whalley and W. G. Schneider, "Compressibility of Gases VIII. Krypton in the Temperature Range 0^{o} to 600^{o}C and Pressure Range 10-80 atm", Trans. ASME, vol. 76, pp.1001-04, August 1954.

10. E. J. Owens and G. Thodos, "Thermal Conductivity - Reduced-State Correlation for the Inert Gases", AIChE Journal, vol. 3, No. 4, pp.454-61, December 1957.

11. V. K. Saxena and S. C. Saxena, "Thermal Conductivity of Krypton and Xenon in the Temperature Range 350-1500K", J. Chem. Phys., vol. 51, pp. 3361-68, October 1969.

12. R. Tufeu, B. LeNiendre, and P. Burg, "High Pressure Thermal Conductivity of Krypton", J. Acad. Sci. Paris, Vol. B273, pp. 61-4, 1971.

13. R. P. Tye, Ed., Thermal Conductivity, Vol. 1, Academic Press, New York, NY, (1969). A. W. Pratt, "Heat Transmission in Law Conductivity Materials".

14. R. G. Deissler and J. S. Boegli, "An Investigation of Effective Thermal Conductivities of Powders in Various Gases", Trans. ASME, vol. 80, pp.1417-25, October 1958.

15. R. Krupiczka, "Analysis of Thermal Conductivity in Granular Materials", Int. Chem. Eng., vol. 7, pp.122-44, January 1967.

16. W. D. Kingery, J. Francl, R. L. Coble, and T. Vasilos, "Thermal Conductivity: X Data for Several Pure Oxide Materials Corrected to Zero Porosity", J. Amer. Ceram. Soc., vol. 37, pp. 107-10, February 1954.

17. D. W. Breck, "Zeolite Molecular Sieves", J. Wiley and Sons, New York NY, 1974.

18. R. C. Weast, Ed., Handbook of Chemistry and Physics, CRC Press, Cleveland, Ohio, 1974.

19. Y. S. Touloukian, Ed., "Thermal Conductivity-Nonmetallic Solids", Thermophys. Prop. Matter, TPRC Data Series, vol. 2, Plenum, NY, 1970.

20. R. H. Perry and C. H. Chilton, Chemical Engineer's Handbook, 5th Ed., McGraw-Hill, New York, NY, 1973.

21. R. A. Brown, Ed., "Krypton Storage Facility", Reference Facility Description for the Recovery of Iodine, Carbon, and Krypton from Gaseous Wastes, ICP-1126, Idaho National Engineering Laboratory, Idaho Falls, ID, to be published 1977.

22. B. A. Foster and D. T. Pence, An Evaluation of High Pressure Steel Cylinders for Fission Product Noble Gas Storage, ICP-1044, Idaho National Engineering Laboratory, Idaho Falls, ID, June 1975.

23. Code of Federal Regulations, "Transportation", Title 49, Part 178, December 15, 1975.

24. W. Murgatroyd, Thermal Convection in a Long Cell Containing a Heat Generating Fluid, AERE EDIR 1559, Harwell, Engl., July 1954.

25. Technical Division Quarterly Progress Report, April 1-June 30, 1977, ICP-1123, Idaho National Engineering Laboratory, Idaho Falls, ID, to be published 1977.

26. J. J. Cuomo and R. J. Gambino, "Incorporation of Rare Gases in Sputtered Amorphous Metal Films", J. Vac. Sci. Technol., vol. 14, pp. 152-157, 1977.

27. R. B. Bird, W. E. Stewart, and E. N. Lightfoot, Transport Phenomena, J. Wiley and Sons, New York, NY, 1960.

APPENDIX A

DERIVATION OF HEAT TRANSFER EQUATIONS FOR A SIMPLE INFINITE CYLINDER

The conductivity equation, where the temperature is radially dependent only, has been used.[27] The thermal conductivity, k, will be assumed linearly dependent on temperature, as shown below

$$k = A + B \cdot T \tag{A-1}$$

where A and B are determined experimentally, and T is in K.

The steady-state conduction equation for an infinite cylinder with a constant volumetric heat generation S (in W/cm^3) is

$$\nabla q = Sr \tag{A-2}$$

where q indicates heat flux, in $W/K \cdot cm^2$ and r is the radius in cm. Fourier's law is assumed to be valid, resulting in

$$\frac{d}{dr}(r\ K\ \frac{dT}{dr}) = -Sr \tag{A-3}$$

The boundary conditions are:

1. Zero heat flux at $r = 0$
2. $T = T_1$ at $r = r_1$

where r_1 and T_1 are the cylinder wall radius and temperature, respectively.

The solution of Equation A-3 is:

$$AT + \frac{B}{2} T^2 = \frac{S}{4} (r_1^2 - r^2) + AT_1 + \frac{B}{2} T_1^2 \tag{A-4}$$

Heat transfer through the cylinder wall will be calculated. Such a calculation is not important for storage cylinders where wall thickness is small.

$$T_1 - T_2 = \frac{r_1 q_1}{k_w} \ln(r_2/r_1) \tag{A-5}$$

where T_2 and r_2 are the outside wall boundary temperature and radius, respectively, and k_w is the wall conductivity.

Heat convects from the outside wall to the air. Newton's Law expresses the dependence of the wall flux (q_2) on the wall temperature gradient

$$q_2 = h(T_2-T_a) \qquad \text{(A-6)}$$

where T_a is the bulk cooling fluid temperature. The heat transfer coefficient h depends on the fluid, its temperature and pressure, and the wall temperature. Equation A-6 has to be solved numerically to provide T_2.

APPENDIX B

HEAT TRANSFER CORRELATIONS

The heat transfer coefficients for natural convection are dependent on the orientation of the surface and the bulk properties of the cooling fluid, density, thermal conductivity, buoyancy, and viscosity. Data for heat transfer coefficients have been correlated in nondimensional form using the Nusselt (Nu) Grashof (Gr) and Prandtl (Pr) numbers. The data for natural and forced convection were taken from Bird et al.[27] For heat transfer coefficients from a horizontal cylinder, the following relation holds for values of log (GrPr) in the range 0 - 9.

$$\log (Nu) = .0203 + .1284 \log (GrPr) + .0106 \log^2 (GrPr) \qquad (B\text{-}1)$$

For heat transfer from vertical plates or cylinders, the following equation holds for values of log (GrPr) in the range 1 - 11. The correlation is

$$\log (Nu) = .13388 + .1363 \log (GrPr) + .00882 \log^2 (GrPr) \qquad (B\text{-}2)$$

APPENDIX C

PHYSICAL PROPERTIES OF AIR AND WATER

Air

Properties of air have been found at pressures of around 0.1 MPa,[27] and the pressure dependence of viscosity and thermal conductivity has been ignored. Air was assumed to obey the ideal gas law. Data for thermal conductivity and viscosity were obtained from Perry's Handbook.[20]

The thermal conductivity is linear over a large range of temperatures, and the correlation is given below, with k in the range 250 - 450 K.

$$k = 7.6 \times 10^{-7}T + 3.28 \times 10^{-5} \qquad \text{(C-1)}$$

The viscosity data were fitted using the Sutherland equation over the same temperature range as for the thermal conductivity,

$$\mu = \frac{1.456 \times 10^{-5}T^{1.5}}{111 + T} \qquad \text{(C-2)}$$

where μ is in poise.

Water

Pressure is assumed to have a negligible effect on water properties. Models for data fitting were found in Perry.[20] Data in the temperature range 273-373 K were used.[20]

The thermal conductivity in W/cm·K is given as

$$k = 9.6 \times 10^{-3} - 1.06/T \qquad \text{(C-3)}$$

with an r-square factor of 0.98 for the data fit.

The viscosity is given by Equation C-4, where μ is in poise. The r-square factor for the correlation of the data is 0.99.

$$\mu = 1.79 \times 10^{-5} \exp [1866/T] \qquad \text{(C-4)}$$

The density of water may be fitted to a quadratic in temperature, with an r-square value of 0.99

$$\rho = 0.75 + 1.88 \times 10^{-3}T - 3.55 \times 10^{-6}T^2 \qquad \text{(C-5)}$$

where ρ is in g/cm^3. The heat capacity is 4.2 J/g·K.